Mean-field-like structural phase transition of H in Fe/V(001) superlattices



2005 J. Phys.: Condens. Matter 17 2073

(http://iopscience.iop.org/0953-8984/17/13/007)

INSTITUTE OF PHYSICS PUBLISHING JOURNAL OF PHYSICS: CONDENSED MATTER

J. Phys.: Condens. Matter **17** (2005) 2073–2084 doi:10.1088/0953-8984/17/13/007

# Mean-field-like structural phase transition of H in Fe/V(001) superlattices

**Stefan Olsson**[1], **Anna Maria Blixt and Björgvin Hjörvarsson**

Materials Physics, Uppsala University, 751 21 Uppsala, Sweden

E-mail: stefan.olsson@fysik.uu.se

Received 26 October 2004, in final form 17 February 2005
Published 18 March 2005
Online at stacks.iop.org/JPhysCM/17/2073

**Abstract**

We present the hydrogen (H) solubility isotherms in biaxially compressed and elastically constrained quasi-two-dimensional V lattices. The relative partial enthalpy and entropy, as determined from the isotherms, show a temperature dependence for [H/V] $\lessapprox$ 0.1 (atomic ratio). This has not previously been reported for H in bulk V and indicates the presence of strong H–H correlations. For [H/V] $\lessapprox$ 0.1, the H–H interaction was determined to be roughly three times more attractive than in bulk V. The compressibility of the H lattice-gas is derived, and the asymptotic behaviour when approaching the critical point is shown to be in accordance with mean-field theory. The critical temperature and the critical concentration for transition were determined to be $T_C = 251 \pm 1$ and [H/V] $\approx 0.0365$, respectively. The effects of the extension of the lattice and the elastic constraints of the V layers on the H–H interaction and critical behaviour are discussed.

## 1. Introduction

The relation between dimensionality and stability of phases is not yet fully resolved, and continues to motivate new theoretical and experimental research on the subject. Theoretical arguments exclude crystalline order in two dimensions (2D) [1], but permit transitions to short-range ordered phases. Studies of structural phase transitions and critical behaviour in 2D have previously mainly been performed by using adsorbates on solid (or liquid) surfaces. Recent research on hydrogen (H) in superlattices have, however, founded a new experimental playground for addressing questions of this kind. A superlattice composed from two metals with very different H solubility, constitutes a stack of quasi-2D H absorbing structures. The phase diagram for the dissolved H is easily accessible through solubility measurements.

[1] Author to whom any correspondence should be addressed.

  

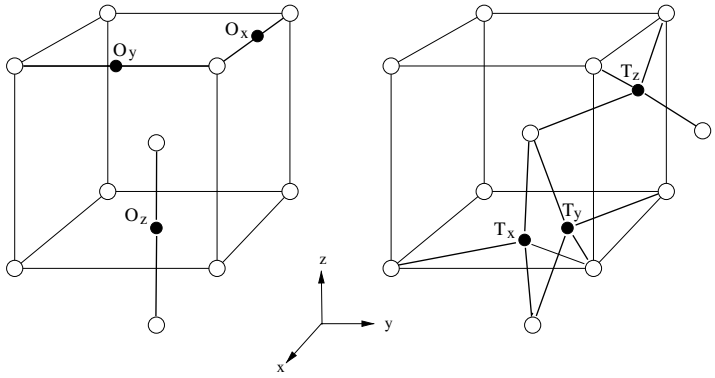


**Figure 1.** The different interstitial sites occupied in Fe/V superlattices. Tetrahedral sites (T) and octahedral sites (O). Whereas the local strain field is close to isotropic for T sites, it is uniaxial for O sites.

Lattice-gas to lattice-liquid phase transformations ($\alpha$–$\alpha'$) of H in the transition metals have been the subject of several earlier investigations. The pioneering work within this field is due to Alefeld [2], who proposed that the transition is driven by long-range elastic interaction between the dissolved H (H–H interaction). Wagner and Horner [3, 4] assumed an interaction of this type and developed the statistical mechanics for the corresponding phase transition. They especially pointed out that the elastic H–H interaction is of Curie–Weiss type (infinite-range) and that for a coherent crystal, macroscopic and shape-dependent H density modes are developing when the phase boundary is crossed. The macroscopic modes were later experimentally verified in single crystals of Nb [5]. Detailed studies of the critical behaviour of H in Pd were carried out by Buck and Alefeld [6], and Ribaupierre and Manchester [7] (PdAg). Both studies resulted in mean-field critical exponents, in the latter study as close as $T/T_C - 1 \approx 10^{-3}$. Since the mean-field approximation is exact for infinite-range interaction, the result was taken as a strong indication that the transition is driven by elastic interaction.

Previous studies of H in Fe/V and Mo/V superlattices focused on the relation between finite-size effects and strain effects of the H uptake [8]. V layers under initial biaxial compressive strain have proved to exhibit an unusually strong attractive H–H interaction in the concentration range [H/V] $\lessapprox 0.1$ (atomic ratio). The strong attractive interaction, as compared to the bulk, is probably the result of the fact that H occupies the $O_z$ sites in the superlattice instead of T sites, which is the normal site occupancy in bulk V. If H is occupying $O_z$ sites in an (001) oriented film, the axes of the local strain fields are aligned in the out-of-plane direction (i.e. $z$ in figure 1). Since, for the superlattice, the V layers are unable to expand in the film plane, a larger part of the local strain can propagate to the sample edges if $O_z$ sites are populated, as compared to T site occupancy. Consequently, an $O_z$ occupancy also implies a larger lattice expansion and a stronger attractive H–H interaction [9]. Moreover, recent experiments point out the possibility of a second-order phase transition within this concentration range [10]. The purpose of the current communication is to investigate the validity of the Curie–Weiss law for H–H interactions in a quasi-2D host lattice and to exploit the possibility of dimensionality crossover. The H solubility isotherms in the solid solution range and in the vicinity of the critical concentration are presented. Furthermore, the compressibility of the H lattice-gas is deduced from the isotherm and its divergence, when approaching the critical temperature, is explored. We also discuss the van't Hoff analysis of the isotherms, which reveals a strong

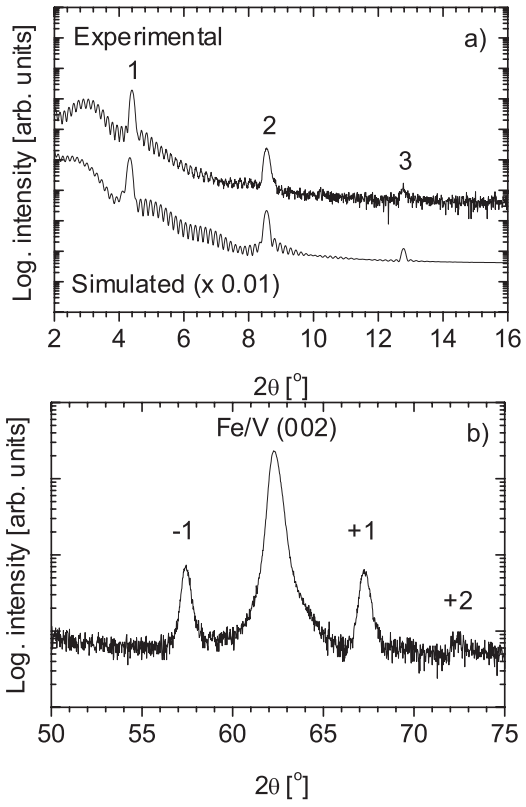


**Figure 2.** (a) The x-ray reflectivity from a virgin Fe/V superlattice. The orders of the superlattice peaks are indicated in the figure. The broadening of the peaks for higher angles is negligible, indicating well defined layer thickness. The result from the simulated reflectivity is further discussed in section 2.1. (b) The high-angle x-ray diffraction pattern from the same sample. The high-angle superlattice satellites are denoted as $\pm n$, $n = 1, \ldots, 2$.

temperature dependence of the enthalpy and entropy of solution in the low concentration range ([H/V] $\lessapprox 0.1$).

## 2. Experimental details

### *2.1. Sample properties and characterization*

An $Fe_{2ML}/V_{12ML} \times 25$ (ML = monolayer) superlattice was grown on an MgO(001) substrate using magnetron sputtering. For a more detailed description of the sputtering system and growth of Fe/V superlattices, see [11]. The substrate was annealed at approximately 625 °C, at $p < 10^{-10}$ mbar, for 30 min prior to film growth. The sample was grown at 330 °C in an Ar (99.9999%) atmosphere of $6.66 \times 10^{-3}$ mbar. A 50 Å thick Pd layer was deposited on top of the film to prohibit oxidation and to serve as a catalytic activator for H dissociation.

The structural quality of the film was investigated with x-ray reflectivity (XRR), and conventional x-ray diffraction (XRD). Both x-rays studies used Cu K$\alpha$ radiation and a conventional Bragg–Brentano set-up (Siemens/Bruker D5000). The result from the XRR is shown in figure 2(a). In the XRR pattern, thin-film thickness oscillations appear up to 8° in

($2\theta$), indicating small variations in the total thickness of the film. A simulation of the XRR pattern, using the Philips WinGIXA software [12, 13], gives an estimation of the interface roughness, i.e., root mean square deviation from an ideally sharp interface, equal to 2.2 Å, and an average bilayer thickness equal to 20.9 Å. The XRD data, seen in figure 2(b), show the fundamental (002) Bragg peak of the film with 1(2) satellite peaks in the lower (higher) angle range. The full width at half maximum of the rocking curve on the (002) Bragg peak was determined to be 0.6°. 2D reciprocal space mapping around the (002), (112) and (022) Bragg peaks was also performed on a Philips X'Pert MRD. The crystalline coherence length, i.e., the distance over which the positions of the atoms are quantitatively correlated, was deduced to be about 2/5 of the total film thickness (210 Å) in the out-of-plane direction. In the [110] and [020] directions (in-plane), the coherence lengths were estimated to be 280 and 180 Å, respectively. The average out-of-plane and in-plane lattice parameters were determined to be 2.976(5) and 2.963(5) Å, respectively. Applying linear elasticity, assuming in-plane coherency, and using the elastic constants for bulk V, gives an out-of-plane lattice parameter of the V layers equal to 3.08 Å, which yields a $c/a$ ratio of the virgin bct cell of the V layers of $\approx$1.04.

### *2.2. p–c–T measurements*

The solubility isotherms were determined from resistivity measurements in an H gas loading apparatus thoroughly described in [10]. During the experiment, the partial pressure of all other gases except H was below $10^{-9}$ mbar. The relative resistivity change due to H ($\Delta\rho/\rho_0$, where $\rho_0$ is the resistivity at 313 K without H) was measured *in situ* by a DC current-reversal technique using a Keithley 2400 Sourcemeter and a Keithley 2182 Nanovoltmeter [14]. The temperature of the film was measured by a chromel–alumel thermocouple, which was in direct contact with the sample surface. An external heating element connected to a Eurotherm 2408 PID controller regulated the temperature within $\pm$0.1 K. The H gas pressure was monitored by three capacitance diaphragm gauges from CCM, Leybold, and Inficon, with a full-scale of 1, 100, and 1000 Torr, respectively. All pressure gauges had a resolution of 0.1% of full-scale. The H gas used in the experiment, originally of 99.9996% purity, was additionally purified, first using a West Associates Ultrapure H gas purifier, and then through an absorption–desorption cycle in a metal–hydride powder.

The [H/V] atomic ratio can be deduced from the resistivity change of the sample. At low H concentrations, the resistivity change is strictly proportional to the H concentration. At higher concentrations this simple proportionality is lost, which normally originates from one or more of the following sources. (1) H–H correlation can affect the resistivity. The effect will however be negligible if the correlation length of the H structure is much smaller than the mean free path of the electrons. (2) H-induced modifications of the electronic structure can cause a significant change in the resistivity [16]. (3) The fact that H occupies a discrete number of interstitial sites gives rise to a parabolic shape of the resistance change curve [15]. Instead of separating all the above contributions to the resistivity change, $\Delta\rho/\rho_0$ can be expressed as a truncated power series in the [H/V] atomic ratio (here denoted as $x$):

$$\frac{\Delta\rho}{\rho_0} = bx + cx^2. \tag{1}$$

Conversion between resistance and H concentration, based on equation (1), has proved to be feasible for similar superlattices [17, 18]. For very high H gas pressures, the resistivity asymptotically approached a maximum, i.e., $\Delta\rho/\rho_0(\max) = 0.635(5)$. The maximum H concentration of Fe/V(001) superlattices, $x_{\max} \approx 1$, is known from earlier experiments [10, 19], which thereby gives $c = -0.635(5)$ and $b = 1.27(5)$ in equation (1).

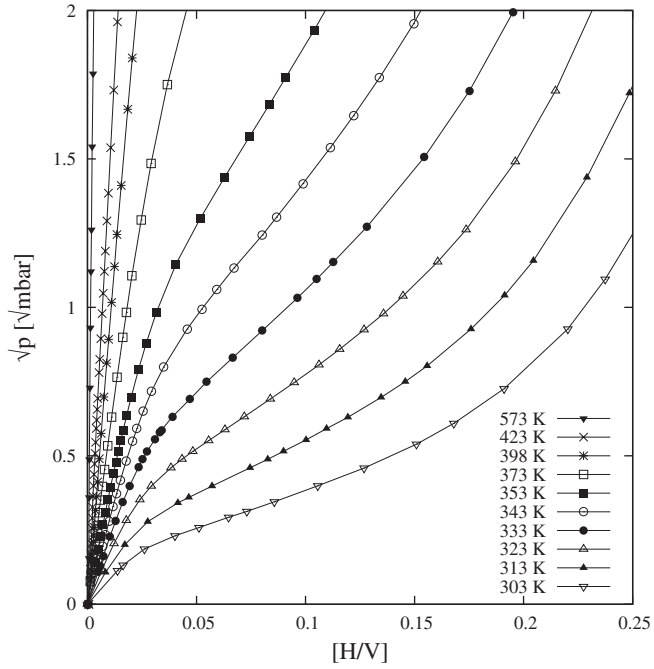


**Figure 3.** The solubility isotherms of H in solid solution in an Fe/V superlattice. The inflection points of the isotherms occur at a concentration which is almost one order of magnitude lower than for bulk V.

## 3. Results and discussion

### *3.1. Solubility isotherms, enthalpy, and entropy*

The H solubility isotherms of the superlattice, as deduced from the resistivity measurements, are presented in figure 3. The solubility in the very low concentration range, i.e., $[H/V] \lessapprox 0.01$, is according to Sievert's law, which means that the concentration is proportional to the square root of the H gas pressure. At higher concentrations, the isotherms clearly deviate from this behaviour and inflection points of the isotherms can, depending on the temperature, be observed in the concentration range $0.05 \lessapprox [H/V] \lessapprox 0.09$. Inflection points of the isotherms are also observed for bulk V [20], but at higher concentrations ($[H/V] \approx 0.25$). For Nb and Pd, the concentration at the inflection point is treated as a marker for the critical concentration for a transition from H lattice-gas to H lattice-liquid. For V, on the other hand, the gas–liquid transition is obscured by the transition to the ordered $\beta$-phase [2]. Within the measured concentration and temperature range, the present sample showed no transition of the latter kind, which is also concluded from previous measurements on the same type of samples. [19, 10].

The pressure dependence of the chemical potential of H gas can be written as

$$\mu_{H_2} = \mu^0_{H_2} + k_B T \ln p, \tag{2}$$

where $\mu^0_{H_2}$ is the chemical potential at the reference pressure (1 atm). At equilibrium, the chemical potentials of H in the gas phase ($\frac{1}{2}\mu_{H_2}$) and the dissolved H ($\mu_\alpha$) are equal, which, using equation (2), gives the following relation [21]:

$$\Delta\mu_H \equiv k_B T \ln \sqrt{p} = \Delta\bar{H}_H - T\Delta\bar{S}_H, \tag{3}$$

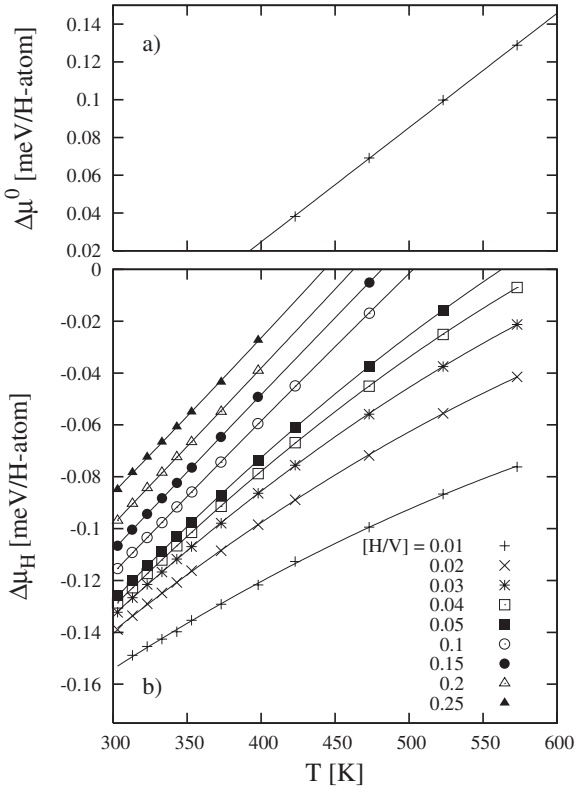


**Figure 4.** (a) A plot of $\Delta\mu^0 \equiv k_B T \ln K_s$, where $K_s$ is Sievert's constant, for H in an Fe/V superlattice. (b) The relative chemical potential of H at various concentrations in the same sample.

where $\Delta\mu_H$, $\Delta\bar{H}_H$, and $\Delta\bar{S}_H$, are the respective relative chemical potential, partial enthalpy, and partial entropy. Plots of $\Delta\mu_H$ versus $T$ at various concentrations are presented in figure 4. Evidently, from the figure, the strict proportionality between $\Delta\mu_H$ and $T$ is no longer valid in the low concentration range (H/V $\lessapprox 0.1$). This is in contrast to previous measurements of the single phase thermodynamics of H in bulk V [22] and thin V layers [17], and implies a temperature dependence in $\Delta\bar{H}_H$ and $\Delta\bar{S}_H$. The temperature dependence of $\Delta\mu_H$ at various concentrations was successfully described with a second-order polynomial in the temperature, shown as the solid lines in figure 4. The enthalpy and entropy could thereby be derived from the chemical potential using the following thermodynamic relations [23]:

$$\Delta\bar{H}_H = \Delta\mu_H - T\frac{\partial\Delta\mu_H}{\partial T} \tag{4}$$

$$\Delta\bar{S}_H = -\frac{\partial\Delta\mu_H}{\partial T}. \tag{5}$$

The deduced relative partial enthalpy and entropy of the dissolved H are presented, at three different temperatures, in figure 5.

The term $-k_B \ln x$, where $x$ is the atomic ratio, is usually subtracted from the entropy in order to avoid a diverging entropy term at low concentrations:

$$\Delta\bar{S}'_H = \Delta\bar{S}_H + k_B \ln x. \tag{6}$$

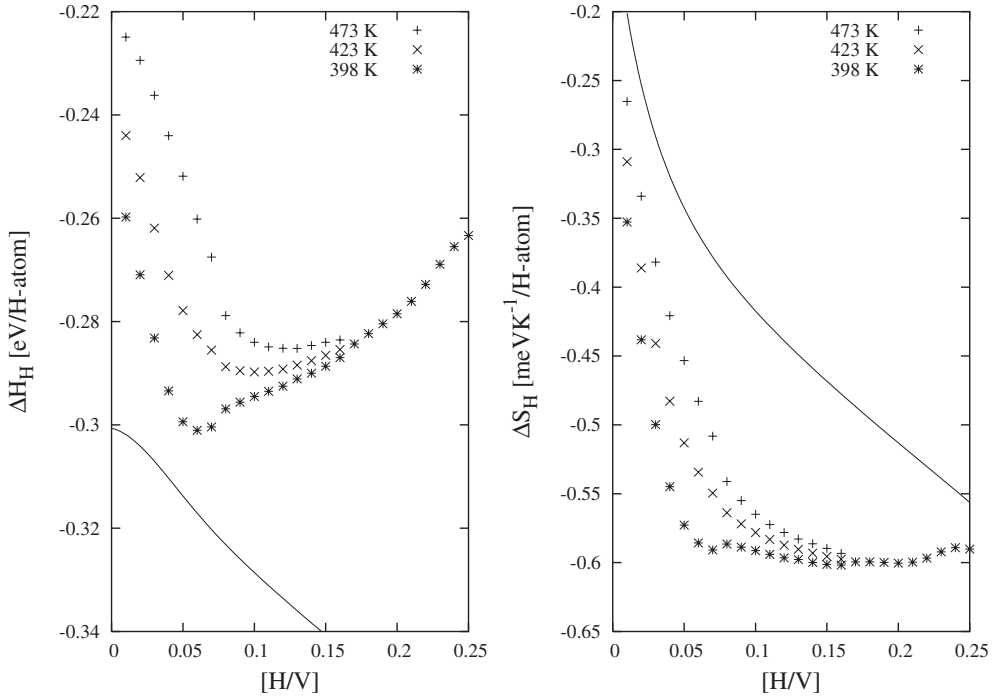


**Figure 5.** The relative partial enthalpy and entropy for H in an Fe/V superlattice at three different temperatures. The solid curves are for bulk V [20].

In the limit $x \to 0$, $\Delta\bar{S}'_{\mathrm{H}} \to \Delta\bar{S}^0_{\mathrm{H}}$, and $\Delta\bar{H}_{\mathrm{H}} \to \Delta\bar{H}^0_{\mathrm{H}}$, which are denoted as the partial enthalpy and entropy of solution at infinite dilution, respectively, and can be deduced from the temperature dependence of Sievert's constant,

$$K_{\mathrm{s}}(T) \equiv \exp\left(\frac{\Delta\bar{H}^0_{\mathrm{H}}}{k_{\mathrm{B}}T} - \frac{\Delta\bar{S}^0_{\mathrm{H}}}{k_{\mathrm{B}}}\right). \tag{7}$$

$K_{\mathrm{s}}$ is obtained from the slope of the isotherms at lowest concentrations and highest temperatures. $\Delta\mu^0 \equiv k_{\mathrm{B}}T \ln K_{\mathrm{s}}(T)$ as a function of temperature is shown for the four highest temperatures in figure 4. Within this temperature range no temperature dependence was noticed in $\Delta\bar{H}^0_{\mathrm{H}}$ and $\Delta\bar{S}^0_{\mathrm{H}}$. From equation (7), the enthalpy and entropy of solution at infinite dilution were determined to be $\Delta\bar{H}^0_{\mathrm{H}} = -0.217(3)$ eV/H-atom and $\Delta\bar{S}^0_{\mathrm{H}} = -7.52(6)k_{\mathrm{B}}$/H-atom, respectively. Compared to bulk V, $\Delta\bar{H}^0_{\mathrm{H}}$ is $\approx$90 meV/H-atom less negative, and $\Delta\bar{S}^0_{\mathrm{H}}$ is changed by $\approx -0.5k_{\mathrm{B}}$/H-atom. The large shift of $\Delta\bar{H}^0_{\mathrm{H}}$ towards a less exothermic reaction compared to the bulk has been discussed elsewhere [10], and is partly due the effect of the biaxial compressive strain of the V cell on the mean interaction potential constituted from the free electrons of the metal.

For the lowest temperatures, where plots of $\sqrt{p}$ versus $x$ are nonlinear even at very low concentrations, the above Sievert's analysis of the isotherms cannot be applied. However, an extrapolation of $\Delta\bar{H}_{\mathrm{H}}$ to zero concentration, and a fit of $\Delta\bar{S}_{\mathrm{H}}$ to equation (6) in the low concentration range, give an estimation of $\Delta\bar{H}^0_{\mathrm{H}}$ and $\Delta\bar{S}^0_{\mathrm{H}}$, respectively. This reveals a temperature dependence in both $\Delta\bar{H}^0_{\mathrm{H}}$ and $\Delta\bar{S}^0_{\mathrm{H}}$. As the temperature is lowered from 473 to 323 K, $\Delta\bar{H}^0_{\mathrm{H}}$ and $\Delta\bar{S}^0_{\mathrm{H}}$ are changing by $\approx -20$ meV/H-atom and $\simeq -0.8k_{\mathrm{B}}$/H-atom, respectively.

Previous investigations of V show that the H-site occupancy can easily be changed by applying strain [24]. It is plausible that the elongation of the *c*-axis of the V-cell in Fe/V(001) superlattices induces a change of site, from tetrahedral (T), which is the normal occupancy in bulk V, to octahedral $z$ ($O_z$) sites. This picture is supported both from the H-induced lattice expansion [25] and from EXAFS measurements [26]. The population of two different sites with a small difference in absorption potential would produce a temperature dependence of $\Delta\bar{H}^0_H$ similar to what is observed for the superlattice. The entropy data also give a hint of which site is more energetically favourable to occupy. $\Delta\bar{S}^0_H$ can be separated in one configurational and one non-configurational term:

$$\Delta\bar{S}^0_H = \Delta\bar{S}^{nc,0}_H + k_B \ln\beta, \tag{8}$$

where $\beta$ is the number of sites per metal atom that are available for occupation, i.e., $\beta = 6$ for T and $\beta = 1$ for $O_z$. The simplest approach is to assume that $\Delta\bar{S}^{nc,0}_H$ is the same as in bulk V, and to attribute the observed shift of $\Delta\bar{S}^0_H$ with temperature to a multiple population of T and $O_z$ sites. This results in a ratio of H occupying $O_z$ sites to the total number of H, which changes from ≈30% to ≈80% if the temperature is reduced from 473 to 323 K.

Within a range of continuous solubility, the change of $\Delta\bar{H}_H$ with concentration can be interpreted to be due to a mean H–H interaction, which at low concentrations is attractive (negative slope) and at higher concentrations repulsive (positive slope). By using a mean-field approach, the enthalpy can be written as

$$\Delta\bar{H}_H = \Delta\bar{H}^0_H + ux, \tag{9}$$

where $u$ is the mean interaction energy. Using equation (9) we can estimate the mean H–H interaction in the superlattice from the initial slope of $\Delta\bar{H}_H$ versus $x$. This gives $u \approx -0.77$ eV/H-atom at 473 K, which is roughly three times more attractive than for bulk V, and as can be seen in figure 5(a), the interaction is even further enhanced at lower temperatures. The adhesion of the film to the substrate, as well as to the H-free layers, constrains the H-induced lattice expansion to occur solely in the out-of-plane direction. As originally pointed out by Alefeld [2], elastic constraints are expected to reduce the elastic H–H interaction. However, within this context it is essential to take into account the symmetry and orientation of the local strain field surrounding the H atom [9]. The symmetry of the local strain field induced by H at $O_z$ sites (see figure 1) is uniaxial, with the axis parallel with the out-of-plane direction, whereas it is nearly isotropic for T sites. Since the layers are unable to expand in the plane the occupation of $O_z$ sites implies a more effective propagation of the strain field to the sample edges. Hence, the strong H–H interaction in the superlattice can be associated with a partial population of $O_z$ sites. The link between H-site occupancy and H–H interactions in the case of 2D elastic constraints is further discussed in [9].

The concentration dependence of $\Delta\bar{S}_H$ reveals a significant deviation from a random distribution already at very low concentration, which is very different from the behaviour in the bulk (see figure 5). The inhomogeneities in the H distribution, which are pronounced at lower temperatures, is a clear sign of H ordering. The general behaviour of H in the superlattice, showing an unusual strong attractive H–H interaction at low concentrations, and a crossover to repulsive H–H interaction at much lower concentrations than for bulk V, is unique for Fe/V(001) superlattices [19, 10]. The H ordering, strong interaction, and the temperature dependence of $\Delta\bar{H}_H$ and $\Delta\bar{S}_H$, clearly manifest a very different H phase behaviour than in bulk V.

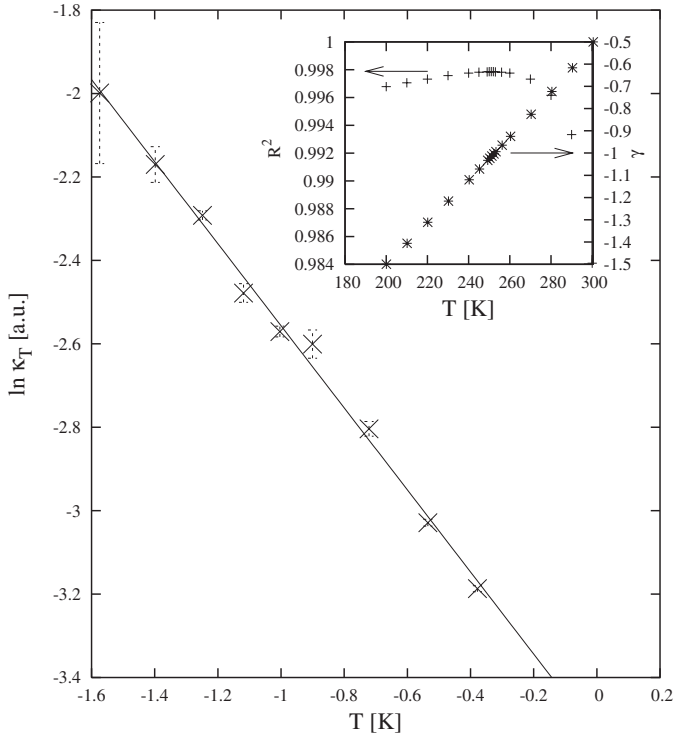


**Figure 6.** The temperature dependence of the isothermal compressibility ($\kappa_T$) of the H lattice-gas evaluated at the points of inflection of the H solubility isotherms in an Fe/V superlattice. The inset show the results from fitting the compressibility according to $\ln \kappa_T = \gamma \ln [T/T_c - 1]$ for different values of $\gamma$ and $T_c$. The largest value for the linear correlation coefficient ($R_2$) corresponds to $T_c = 251 \pm 1$ K and $\gamma = -1.01 \pm 0.01$.

### *3.2. Critical behaviour*

The isothermal compressibility of the H lattice-gas can be determined from the slope of the solubility isotherms [6]:

$$\kappa_T^{-1} \propto x^2 T p^{-1} \left.\frac{\partial p}{\partial x}\right|_{p,T}. \tag{10}$$

When approaching a critical point from above (in temperature) one would expect a diverging compressibility according to

$$\kappa_T \propto t^{-\gamma}, \qquad t \equiv \frac{T}{T_C} - 1. \tag{11}$$

The critical temperature, $T_C$, and the exponent, $\gamma$, are determined from a plot of $\ln \kappa_T$ versus $\ln t$ for different values of $T_C$. The maximum value of the correlation coefficient of a linear fit to the data ($R^2$) occurs with $T_C = 251 \pm 1$ K and $\gamma = 1.01 \pm 0.01$ (see the inset to figure 6), and the corresponding plot for this set of critical parameters is presented in figure 6. The obtained value for $\gamma$ agrees with mean-field theory, and is also in accordance with the corresponding exponent for the $\alpha$–$\alpha'$ transition of H in bulk Pd [7] and Nb [27]. The phase boundary can be determined from the asymptotic behaviour of the isotherms near the critical concentration.

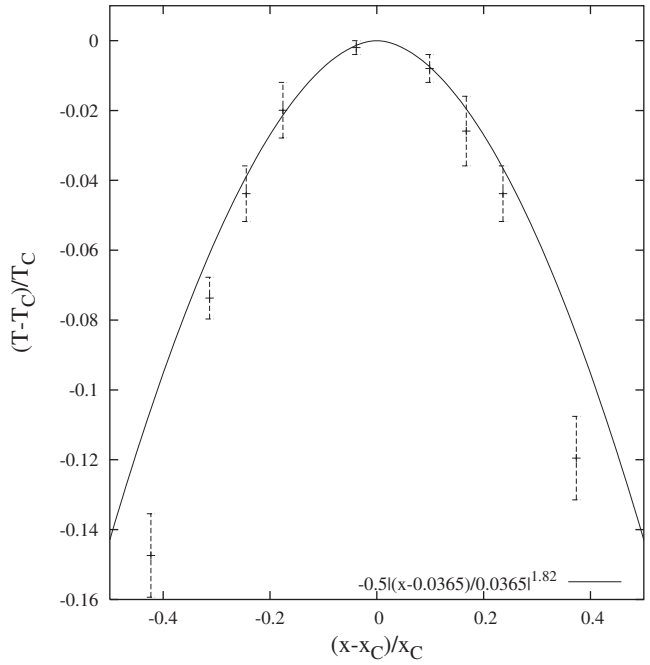


**Figure 7.** The spinodal boundary for H in an Fe/V superlattice. The solid points are deduced from the extrapolation of the fitted isotherms. The solid curve is the fit to the spinodal boundary according to a power law with exponent $1/\beta = 1/0.55$. See the text for details.

From the condition for thermodynamic stability,

$$\frac{\partial \mu_{\mathrm{H}}}{\partial x} \geqslant 0, \tag{12}$$

the boundary to the region of unstable states, i.e., the spinodal, can be identified as when $\partial \mu_{\mathrm{H}}/\partial x = 0$. The change in chemical potential with concentration is easily extracted from the isotherms, i.e.,

$$\frac{\partial \mu_{\mathrm{H}}}{\partial x} \propto \frac{T}{p}\frac{\partial p}{\partial x}\bigg|_{p,T}, \tag{13}$$

and the spinodal boundary at selected concentrations around the critical point is shown in figure 7. The same technique used for determining $\gamma$ and $T_{\mathrm{C}}$ can now be applied to find the critical concentration ($x_{\mathrm{C}}$) and the critical exponent $\beta$. In this case, however, a simple power law was inadequate to fit the spinodal curve. The best fit gives $x_{\mathrm{C}} = 0.0365$ and $\beta \approx 0.55$, and is plotted as the solid curve in figure 7. The obtained value for $\beta$ is in reasonable agreement with the mean-field value ($\beta = 0.5$), and thereby consistent with the findings above. Despite the difficulties in fitting the spinodal curve with a simple power law, the experimental points are symmetric with respect to $x_{\mathrm{C}}$, and one can assume that the value for the critical concentration is accurate. It is worth noticing that the concentration at the critical point is almost one order of magnitude lower than for the corresponding transition in bulk samples of Nb or Pd.

Using a generalized model of the interaction, the temperature range where the classical (mean-field) theory does not apply ($t_{\mathrm{nonclassical}}$) has been estimated by Fisher [28]:

$$t_{\mathrm{nonclassical}} \approx A\left(\frac{a}{b}\right)^{d}. \tag{14}$$

Here $A$ is of the order unity, $a$ is the size of the interacting particles, $b$ is the range of the interaction, and $d$ is the dimensionality. Depending on the value of $t$ at the inflection points, equation (14) gives the lower limit of the range of the H–H interaction:

$$b \gtrapprox 2.2a \text{ (2D)} \tag{15}$$

$$b \gtrapprox 1.7a \text{ (3D)} . \tag{16}$$

A rough estimation of $a$ can be made using the critical concentration and by assuming randomly distributed H. If this value is inserted in equations (15) and (16), we have

$$b \gtrapprox 24 \text{ Å (2D)} \tag{17}$$

$$b \gtrapprox 12 \text{ Å (3D)} . \tag{18}$$

It is obvious from equations (17) and (18) that, regardless of the dimensionality, phase transitions due to macroscopic-range interaction would behave according to the mean-field model infinitely close to the critical temperature. On the other hand, for phase transitions due to finite-range interaction, equations (17) and (18) give a lower limit of the range of the interaction, which is of the order of the thickness of the V layers, i.e., $\simeq$10 Å.

## 4. Conclusion

The enthalpy and entropy data, as deduced from the solubility isotherms, indicate a strong H–H correlation at concentrations as low as [H/V] $\approx$ 0.05, which is in stark contrast to bulk V. The enhanced H–H interaction in Fe/V(001) superlattices has previously been associated with a parallel alignment of the elastic dipoles, as a result of exclusive population of $O_z$ sites. This concept was first brought up by Alefeld [2], but experimental evidence of such behaviour has up to now been scarce. Although the population of $O_x$ and $O_y$ can be excluded, partial occupation of T sites is still possible. We are here arguing that the multiple population of $O_z$ and T sites is causing the temperature dependence seen in $\Delta\bar{H}^0_{\mathrm{H}}$ and $\Delta\bar{S}^0_{\mathrm{H}}$. The concentration dependence of the entropy indicates a strong H–H correlation at low concentration, and for temperatures below $\approx$400 K. The mean-field behaviour of the compressibility and the coexistence curve, however, indicate that the H are correlated over, at least, distances of the order of the V layer thickness. This highlights the importance of long-range elastically mediated interactions in H–metal systems. It is therefore of great interest to explore these effects in samples with smaller extensions of the H absorbing layers, and as close as possible to the critical point. If a dimensional crossover would occur it can give unique information to further understand the mechanism behind the H–H interaction and, more generally, it could provide a new insight in the behaviour of quasi-2D structural phase transitions.

## Acknowledgments

The work was financially supported by the Swedish Research Council, which is gratefully acknowledged. The authors also would like to thank Professor S T Bramwell for his interest and valuable reflections when preparing the paper.

## References

[1] Mermin N D 1968 *Phys. Rev.* **176** 250
[2] Alefeld G 1972 *Ber. Bunsenges. Phys. Chem.* **76** 746
[3] Wagner H and Horner H 1974 *Adv. Phys.* **23** 587
[4] Horner H and Wagner H 1974 *J. Phys. C: Solid State Phys.* **7** 3305

[5] Zabel H and Peisl H 1979 *Phys. Rev. Lett.* **42** 511
[6] Buck H and Alefeld G 1972 *Phys. Status Solidi* b **49** 317
[7] de Ribaupierre Y and Manchester F D 1974 *J. Phys. C: Solid State Phys.* **7** 2126
[8] Hjörvarsson B, Andersson G and Karlsson E 1997 *J. Alloys Compounds* **253** 51
[9] Olsson S and Hjörvarsson B 2005 *Phys. Rev.* B **71** 035414
[10] Olsson S, Blomquist P and Hjörvarsson B 2001 *J. Phys.: Condens. Matter* **13** 1685
[11] Isberg P, Hjörvarsson B, Wäppling R, Svedberg E B and Hultman L 1997 *Vacuum* **48** 483
[12] Paratt L G 1954 *Phys. Rev.* **95** 359
[13] de Boer D K G 1991 *Phys. Rev.* B **44** 498
[14] Olsson S 2003 *PhD Thesis* Uppsala University, Uppsala
[15] Watanabe K and Fukai Y 1980 *J. Phys. F: Met. Phys.* **10** 1795
[16] Meded V, Olsson S, Zahn P, Hjörvarsson B and Mirbt S 2004 *Phys. Rev.* B **69** 205409
[17] Stillesjö F, Olafsson S, Isberg P and Hjörvarsson B 1995 *J. Phys.: Condens. Matter* **7** 8139
[18] Olsson S, Hjörvarsson B, Svedberg E B and Umezawa K 2002 *Phys. Rev.* B **66** 155433
[19] Andersson G, Hjorvarsson B and Isberg P 1996 *Phys. Rev.* B **55** 1774
[20] Veleckis E and Edwards R K 1969 *J. Phys. Chem.* **73** 683
[21] Flanagan T B and Oates W A 1972 *Ber. Bunsenges.* **76** 706
[22] Kleppa O J, Dentzer P and Melnichak M E 1974 *J. Chem. Phys.* **61** 4048
[23] Guggenheim E A 1967 *Thermodynamics* (Amsterdam: North-Holland)
[24] Yagi E, Kobayashi T, Nakamura S, Kano F, Watanabe K, Fukai Y and Koike S 1986 *Phys. Rev.* B **33** 5121
[25] Andersson G, Hjörvarsson B and Zabel H 1997 *Phys. Rev.* B **55** 15095
[26] Burkert T, Miniotas A and Hjörvarsson B 2001 *Phys. Rev.* B **63** 125424
[27] Schnabel D and Alefeld G 1975 *Collect. Phenom.* **2** 29
[28] Fisher M E 1967 *Rep. Prog. Phys.* **30** 615